China Geology 7 (2024) 469–479

China Geology

Journal homepage: http://chinageology.cgs.cn
https://www.sciencedirect.com/journal/china-geology

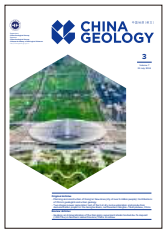

Contamination assessment, source apportionment and associated health risks of PTEs in agricultural soil under five land-use patterns in Sanya, China

Jian-zhou Yang[a, b], Yan-gang Fu[a], Qiu-li Gong[a, b,*], Sheng-ming Ma[a], Jing-jing Gong[a], Jian-weng Gao[a], Zhen-liang Wang[a], Yong-wen Cai[a], Shi-xin Tang[a]

[a] *Institute of Geophysical and Geochemical Exploration, Chinese Academy of Geological Sciences, China Geological Survey, Langfang* 065000, *China*
[b] *Key Laboratory of Coupling Process and Effect of Natural Resources Elements, Ministry of Natural Resources, Beijing* 100055, *China*

ARTICLE INFO

Article history:
Received 16 March 2021
Received in revised form 21 February 2022
Accepted 27 April 2022
Available online 18 September 2023

Keywords:
Potentially toxic trace elements (PTEs)
Soils
Land-use
Geo-accumulation index (I_{geo})
Hazard quotient (HQ)
Total carcinogenic risk index (TR)
Source apportionment
Health risk
Agricutural geological survey engineering

ABSTRACT

To understand the levels of potentially toxic elements (PTEs) contamination in soils and their effects on human health from different agricultural land use in Sanya, China. 128 soil samples (64 topsoil samples and corresponding subsoil samples) were collected from the five representative land-use patterns. Inductively coupled plasma mass spectrometry (ICP-MS), Atomic fluorescence spectrometry (AFS), and Inductively coupled plasma optical emission spectrometry (ICP-OES) were used to determine the content of PTEs (As, Cd, Hg, Cu, Cr, Ni, Pb, Zn, Co, Mo, Sb, and V). Correlation analysis and factor analysis were used to determine the source of PTEs. Geo-accumulation index (I_{geo}), hazard quotient (HQ), and total carcinogenic risk index (TR) were used to measure the PTEs contamination and its relative health impacts. Results showed that the average values of 12 PTEs in topsoil were higher than the Hainan soil geochemical baseline, showing different degrees of PTEs accumulation effect. The concentration of PTEs in the topsoil was lower than those in the subsoil except for Cd and Hg. The I_{geo} revealed that the major accumulated element in soils was As followed by Mo. Source apportionment suggested that parent materials and agricultural practices were the dominant factors for PTEs accumulation in the topsoil. Non-carcinogenic risks of soil samples from five land-use patterns presented a trend of paddy field > dry field > woodland > orchard > garden plot. However, the HQ values of 12 PTEs were less than the recommended limit of HQ = 1, representing that there are no non-carcinogenic risks of PTEs for children and adults in the study area. The TR values are within 6.95×10^{-6}–1.38×10^{-5}, which corresponds to the low level. Therefore the PTEs in the agricultural soil of the study area show little influence on the health status of the local population.

1. Introduction

Soil is a critical component for both agricultural production and human survival. However, with the rapid growth of the global population, particularly driven by the swift expansion of urbanization and industrialization, there has been a heightened focus on soil pollution (Pourret O et al., 2018). Among the various contaminants found in soil, potentially toxic elements (PTEs) stand out due to their persistent nature, high toxicity levels, and enduring presence in the environment (Kim HS et al., 2015; Geng N et al., 2019). The excessive accumulation of PTEs, whether caused by natural environmental changes or human activities, poses a significant threat not only to ecosystems but also to human health. PTEs can enter the human body through multiple pathways, including ingestion, inhalation, and dermal contact (Liu H et al., 2018; Ali L et al., 2019). For instance, the over-absorption of Pb can result in anemia and kidney diseases, adversely affecting the endocrine and immune systems. The accumulation of Cd in the human body may lead to lung diseases, prostate disorders, renal insufficiency, or various bone-related conditions through its interaction with Ca. Furthermore, the presence of As and Hg in the human body can lead to skin problems, peripheral nerve damage, vascular diseases, and, in some cases, even lung and liver cancer (Zhang XW et al., 2012; Cao SZ et al., 2013; Timofeev I et al., 2019).

In a broader context, the presence of PTEs in natural soil environments is influenced by geological factors, including the soil 's parent material and its pedogenic development

First author: *E-mail address*: yjianzhou@mail.cgs.gov.cn (Jian-zhou Yang).

* Corresponding author: *E-mail address*: gqiuli@mail.cgs.gov.cn (Qiu-li Gong).

Literary editor: Li-qiong Jia
doi:10.31035/cg2023078
2096-5192/© 2024 China Geology Editorial Office.

process (Micó C et al., 2006; Wang AT et al., 2018). Additionally, human activities such as agriculture, mining, and industrial emissions represent significant sources of PTEs (Yin YM et al., 2018; Bao LR, 2020; Fei XF et al., 2020; Wang FF et al., 2020), often contributing more PTEs to the environment than natural sources (Yang SH et al., 2020). Among these activities, the type of land utilization plays a crucial role in determining PTE levels in soil, with agricultural lands being particularly susceptible. The application of chemical fertilizers, insecticides, herbicides, and intensive management practices such as mulching and greenhouse cultivation can accelerate the accumulation of PTEs in agricultural soil (Qishlaqi Y et al., 2009; Deng Y et al., 2019; Fei XF et al., 2020; Liu HW et al., 2021). Considering the direct and indirect impacts of agricultural soil on public health through food production, it is essential to gain a comprehensive understanding of the concentrations, sources, and associated health risks of PTEs in agricultural soil.

Sanya, located in the southern part of Hainan province (Fig 1), China, is a globally renowned tourist city where agricultural production plays a vital role in the local economy. In contrast to mainland China, Sanya 's soil remains predominantly unpolluted due to limited industrial activities (Wang AT et al., 2018), making it an ideal location for investigating the characteristics of PTEs in agricultural lands. Furthermore, with the implementation of the national ecological civilization pilot zone scheme in Hainan by the Chinese government, agricultural soil security has become a prominent concern. While factors such as industry and tourism can potentially influence PTE levels in soils (Timofeev I et al., 2017; Memoli V et al., 2019), this study primarily seeks to identify the primary sources of heavy metals through elemental correlations due to data limitations. The research focuses on five categories of agricultural lands in the Sanya region, utilizing geological statistics and the hazard coefficient method (USEPA, 2002) to compare the characteristics of PTEs in agricultural soil under various land utilization patterns. Additionally, the study aims to assess the potential health risks for residents posed by the topsoil. Ultimately, this research endeavors to provide scientific guidance for the prevention and mitigation of ecological risks associated with soil PTEs and to advance environmental preservation efforts.

2. Study area

As depicted in Fig 1, Sanya is situated in the southern region of Hainan, China, positioned between 18°09′34″ to 18°37′27″ north latitude and 108°56′30″ to 109°48′28″ east longitude. It shares borders with Lingshui to the east, Baoting County to the north, and Ledong County to the west, and is bounded by the South China Sea to the south, encompassing an approximate land area of 1919 km^2. Geographically, Sanya exhibits a variation in terrain, characterized by higher elevations in the north, gradually transitioning to lower elevations in the south. This region experiences a tropical maritime monsoon climate, featuring an annual average

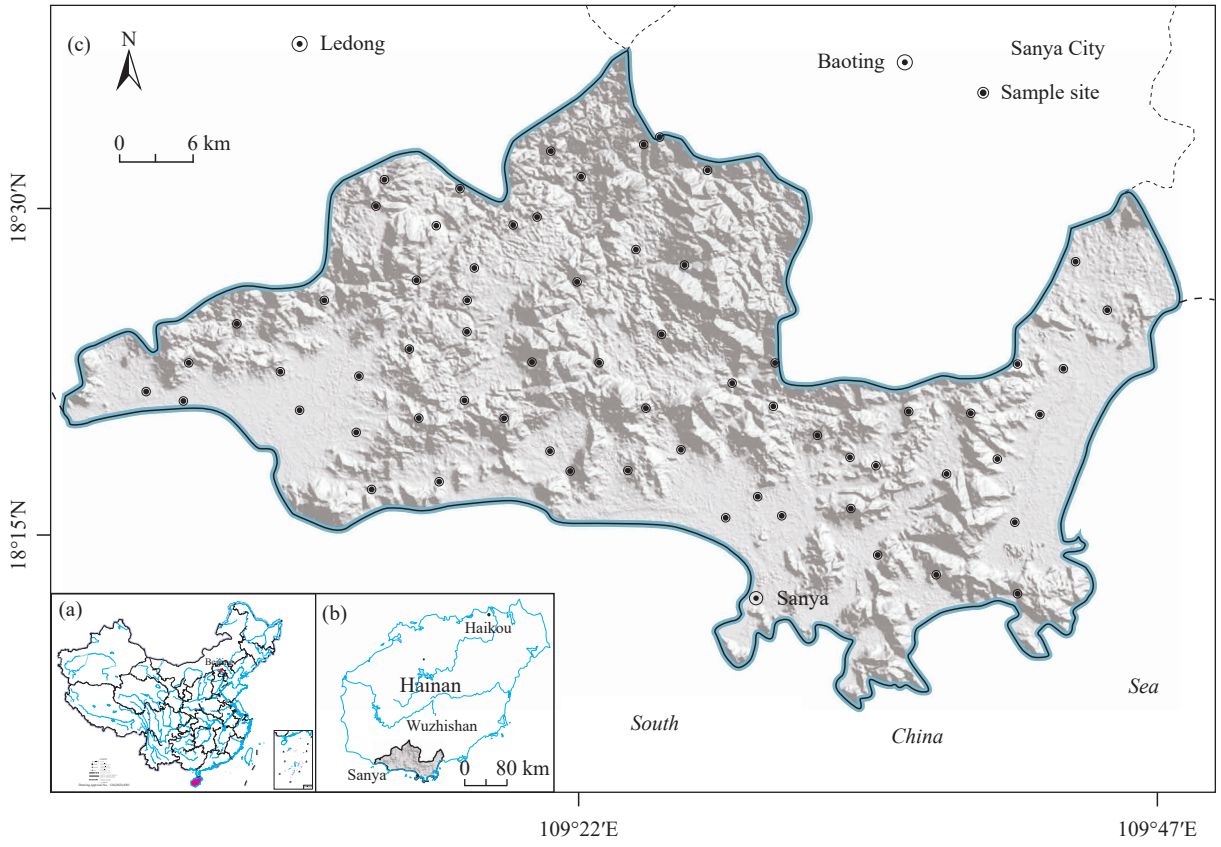

Fig. 1. a–Location of Hainan Island within China (basemap after China National Bureau of Surveying and Mapping Geographical Information); b–location of the Sanya region; c–distributions of sampling sites.

temperature of 25.7°C, an annual sunshine duration of 2534 hours, and an annual precipitation of 1347.5 mm. The agricultural lands within this area are categorized into five distinct types, namely paddy fields, dry land, orchards, garden plots, and woodland.

3. Samples and analytical methods

3.1. Sample collection

Following the land utilization type map of the Sanya region, soil samples were meticulously collected for analysis, taking into account the distribution of various agricultural land types. Sampling points were carefully chosen in areas characterized by level terrain, thick soil layers, and an absence of evident anthropogenic pollution. To ensure representative sampling, the authors employed a motorized shallow drilling machine to extract soil columns extending to a depth of two meters. Subsequently, a bamboo knife was employed to separate the soil adhering to the stainless steel drill pipe. From the extracted soil columns, two distinct samples were obtained: One from the 0–25 cm depth and another from the 175–200 cm depth. These samples were carefully placed into clean sample bags. Subsequently, the samples were subjected to air-drying within a laboratory setting and sifted using a 10-mesh nylon sieve. For testing purposes, 200 g of the sifted soil from each sample was selected. In total, 128 soil samples were gathered from 64 sampling points, with representation from orchards (n=21), dry land (n=11), woodland (n=6), garden plots (n=21), and paddy fields (n=5).

3.2. Analytical methods

Chemical analyses were carried out at the central laboratory of the North China Geological Exploration Bureau in Langfang. The collected samples were ground to a fineness of 200 mesh within the laboratory and securely stored for future utilization. Detailed procedures for sample pre-processing, analysis, detection, and quality control can be found in Zhang Q (2012). For the determination of PTE content, a combination of analytical techniques was employed, including Inductively Coupled Plasma Mass Spectrometry (ICP-MS), Atomic Fluorescence Spectrometry (AFS), and Inductively Coupled Plasma Optical Emission Spectrometry (ICP-OES). Additionally, the analysis of Corg and pH levels was conducted using an infrared carbon-sulfur meter (Acid-Base Titration Volumetric Method, VOL) and a pH meter (Ion-Selective Electrode Method, ISE), respectively. Specific analysis methods and detection limits are outlined in Table 1. To ensure the accuracy and precision of our analyses, certified reference materials (GBW07389−GBW07391) were employed for calibration, resulting in accuracy and precision rates exceeding 98%. The detectability of the 12 PTEs under examination was found to be 100%.

Table 1. Analytical methods (AM) and detection limits (DL) of various parameters.

Index	AM	DL	Unit
As	AFS	0.5	mg/kg
Cd	ICP-MS	0.02	mg/kg
Hg	AFS	0.0005	mg/kg
Cu	ICP-MS	1	mg/kg
Pb	ICP-MS	1.5	mg/kg
Zn	ICP-OES	2	mg/kg
Co	ICP-MS	1	mg/kg
Cr	ICP-OES	3	mg/kg
Ni	ICP-MS	1	mg/kg
Mo	ICP-MS	0.3	mg/kg
Sb	AFS	0.05	mg/kg
V	ICP-OES	5	mg/kg
Th	ICP-OES	2	mg/kg
Corg	VOL	0.03	%
pH	ISE	0.1	–

4. Contamination and risk assessment

4.1. Assessment of PTEs pollution in soil

In the context of soil pollution assessment, several common indices, such as the Global Pollution Index, Global Dispersion Index (Kasimov N et al., 2016; Timofeev I et al., 2017), and I_{geo} (Muller G, 1969), are employed to gauge the accumulation levels of Potentially Toxic Elements (PTEs) in soil. In this study, the authors utilized the I_{geo} value, widely applied for soil pollution assessment (Fei XF et al., 2019; Timofeev I et al., 2019; Liu HW et al, 2021), to estimate the contamination of agricultural soils. The I_{geo} index is calculated as follows (Equ 1):

$$I_{geo} = \log_2\left[\frac{C_i}{1.5\times C_b}\right] \quad (1)$$

Where C_i represents the PTE content in agricultural soils, and C_b signifies the geochemical baseline for that specific PTE element within Hainan Province, as determined by the Hainan Geological Survey Institute (Fu YR et al., 2008).

4.2. Assessment of concentration enrichment factor (CEF)

The Concentration Enrichment Factor (CEF) is a valuable metric for distinguishing the impact of enrichment or depletion of PTEs in topsoil (Ansari AA et al., 2000; Fergusson JE, 1990). Its calculation is expressed by the following equation (Equ 2):

$$\mathrm{CEF} = \frac{\left(\frac{Ci}{Cn}\right)\mathrm{Topsoil}}{\left(\frac{Ci}{Cn}\right)\mathrm{Subsoil}} \quad (2)$$

Where Ci represents the measured values of PTEs, while Cn represents the background concentrations of selected reference elements. For the computation of CEF values, elements with limited mobility, such as Nb, Ta, Th, Zr, Hf, Sc, and Ti, are typically employed as reference elements (Nesbitt HW, 1979; Hill IG et al., 2000; Kurtz AC et al., 2000; Wang AT et al., 2018). In this study, the authors designated Thorium (Th) as the reference element, known for its relative stability during the pedogenic process (Braun JJ, 1993).

4.3. Health risk assessment

A health risk assessment of PTEs in soil is conducted for both adults and children using the exposure evaluation model developed by the United States Environmental Protection Agency (USEPA). This model calculates the Average Daily Doses (ADD) of PTE-contaminated topsoil particles based on three exposure pathways: ingestion, dermal absorption, and inhalation (Means B, 1989; USEPA, 2002). Among these pathways, ingestion and dermal absorption are the primary mechanisms for exposure to PTEs in soil (Fryer M et al., 2006; Qu CS et al., 2012). The ADD index is determined by the following formula (Equs 3, 4):

$$ADD_{ingest}=\frac{C_i\times IngR\times EF\times ED}{BW\times AT}\times 10^{-6} \quad (3)$$

$$ADD_{dermal}=\frac{C_i\times SA\times AF\times ABS\times EF\times ED}{BW\times AT}\times 10^{-6} \quad (4)$$

Where ADD_{ingest} and ADD_{dermal} represent the average daily doses through ingestion and dermal absorption, respectively, and C_i denotes the PTE content in topsoil. Table 2 provides details on other parameters, their descriptions, and values.

The HQ is employed to characterize non-carcinogenic hazards and is defined as the ratio of the Chronic Daily Intake (CDI) to the Reference Dose (RfD) (Equs 5, 6):

$$HQ=\sum(HQ_{ingest}+HQ_{dermal})=\sum\left(\frac{ADD_{ingest}}{RfD_o}+\frac{ADD_{dermal}}{RfD_{ABS}}\right) \quad (5)$$

$$RfD_{ABS}=RfD_o\times ABS_{GI} \quad (6)$$

Where HQ_{ingest} and HQ_{dernal} represent the non-carcinogenic hazard quotient through ingestion and dermal absorption, respectively. RfD_o and RfD_{ABS} denote the reference doses for ingestion and dermal absorption, respectively, while ABS_{GI} refers to the absorption efficiency for the PTE. If HQ is below 1, it indicates no significant risk of adverse health effects. Conversely, if HQ exceeds 1, non-carcinogenic effects may become evident. The reference doses for Pb and Mo are based on RSL, 2017, while the other ten PTEs rely on MEP, 2014.

Among the PTEs considered, namely As, Cd, Cr, and Pb, some have been identified as human carcinogens. The Total Risk (TR) associated with the development of tumors due to these metals, taking into account different routes of intake, is calculated as follows (Equs 7, 8):

$$TR=\sum CR_i=\sum(ADD_{ingest}\times SF_o\times ADD_{dermal}\times SF_{ABS}) \quad (7)$$

$$SF_{ABS}=SF_o/ABS_{GI} \quad (8)$$

Where CR_i represents the carcinogenic risks posed to human health by each metal. The slope factors for oral intake are as follows: 1.5 for As, 0.5 for Cr, 15 for Cd, and 0.0085 for Pb (RSL, 2017). SF_{ABS} represents the dermally adjusted slope factor. In general, CR_i values falling within the range of 10^{-4} to 10^{-6} are considered acceptable (Yin YM et al., 2018). TR indices are classified into five levels: Very low ($< 10^{-6}$), low ($10^{-6} – 10^{-5}$), medium ($10^{-5} – 10^{-4}$), high ($10^{-4} – 10^{-3}$), and very high ($> 10^{-3}$) cancer risks (Fryer M et al., 2006; Timofeev I et al., 2019).

5. Results and discussion

5.1. PTEs concentration in the topsoil

The content of PTEs in the topsoil within the study area (Table 3) follows the sequence from highest to lowest as Zn > V > Pb > Cr > Cu > Co > Ni > As > Mo > Sb > Cd > Hg. All of these PTEs exceeded the geochemical baseline values of soil in Hainan Island, as reported by Fu YR et al., (2008). This indicates that the 12 PTEs had accumulated to some extent in the soil. Specifically, the As content ranged from 0.52 mg/kg to 29.9 mg/kg, with an average of 3.80 mg/kg, which is 3.3 times higher than the baseline for soil in Hainan Island. The average Mo content was 1.21 mg/kg, which is 2.4 times higher than the baseline value. For the remaining 10 PTEs, such as Zn, V, Pb, and Cr, their content ranged from 1 time to 1.5 times the baseline values for the soil. Clearly, the cumulative effect of As in the soil was the most significant.

However, according to the national risk control standard (GB15618-2018) for soil contamination in agricultural land, the content of Cd, Hg, As, Pb and Cr in the topsoil across the

Table 2. Exposure parameters of PTEs.

Parameter	Description	Unit	Adult	Child	Reference
IngR	Amount of ingested soil	mg/d	100	200	MEP, 2014
EF	Exposure frequency	d/a	350	350	MEP, 2014
ED	Exposure duration	a	30	6	USEPA, 2002
BW	Average body weight of human	kg	56.8	15.9	MEP, 2014
AT	Average time of exposure for elements	d	Carcinogenic value is 26280, Non-carcinogenic value is 10950	Carcinogenic value is 26280, Non-carcinogenic value is 2190	USEPA, 2002
SA	Skin surface area in contact with soil	cm^2	2415	1295	MEP, 2014
AF	Adherence factor of soil to skin	$mg/cm^2/d$	0.2	0.2	MEP, 2014
ABS	Absorption efficiency for the PTE	–	0.001	0.001	MEP, 2014

five types of agricultural land consistently fell below the risk intervention values. Similarly, the content of Cu, Ni, and Zn was below the risk screening values. The organic carbon content in the samples ranged from 0.22% to 2.16%, and the pH values varied from 4.94 to 7.14, indicating that the soil was weakly acidic to neutral. Previous studies have demonstrated that soil pH values and organic matter content can significantly influence PTE content in soil (Cai LM et al., 2019; Liu HW et al., 2021). The former can affect the chemical forms of PTEs, while the latter has a strong affinity to adsorb PTEs, particularly forming stable complexes with transition elements (Bloom PR et al., 1996; Qishlaqi A et al., 2009), thus impacting PTE content in the soil. Surprisingly, there was no strong correlation observed between soil pH values and PTE content in agricultural lands (Fig. 2). The limited variation range and variance of soil pH values may have contributed to this lack of correlation (Qishlaqi A et al., 2009). Organic matter exhibited varied correlations with different PTEs in various land types: It was insignificantly correlated with Hg, Cu, Zn, and V in orchards, positively correlated with Hg in dry land, significantly positively correlated with As, Cd, Cr, Ni, Sb, and V in woodland, insignificantly related to V, Cr, and Ni in garden plots, and insignificantly correlated with PTE content in paddy fields (Fig. 2). Correlation analysis indicated that organic matter had varying degrees of impact on the soil PTE content in orchards, dry land, woodland, and garden plots.

To determine the priority enrichment elements for each land type, the geochemical baseline of the soil in Hainan Island (Fu YR et al., 2008) was used as a reference standard to evaluate the I_{geo} index. As shown in Fig. 3, As and Mo exhibited varying degrees of enrichment in soils across different land utilization types, with the highest levels found in paddy fields, where their I_{geo} reached 4.1 and 2.1, respectively. Additionally, Cu, Co, and Sb were also enriched to some extent in paddy soil, suggesting a more significant impact on the enrichment of these PTEs in paddy fields. Moreover, Hg displayed higher values in garden plots, with an average I_{geo} of 1.3, indicating its enrichment to a certain extent in garden plot soil. For the remaining PTEs, their average I_{geo} values were below 0, signifying a lower degree of enrichment in agricultural lands.

5.2. Vertical characteristics of soil PTEs and their indication of sources

The characteristics of PTEs in soil exhibit distinct vertical patterns, reflecting their sources and interactions within the soil profile. Topsoil represents the zone most influenced by atmospheric, hydrospheric, and biospheric interactions, while subsoil is typically less affected by human activities. As a result, PTE content in subsoil can serve as a reference value for the initial parent material (Ansari AA et al.,2000; Reimann C et al.,2001). In the subsoil samples, V exhibited the highest average value, followed by Zn (Table 3). Generally, due to human activities, PTEs tend to be enriched in the topsoil (Qishlaqi A et al., 2009; Reimann C et al., 2001). Surprisingly, in this study, aside from Cd and Hg, which had slightly higher concentrations in the topsoil, the content of the other 10 PTEs was found to be higher in the subsoil (Table 3). This unusual pattern could be attributed to the unique geographical environment on Hainan Island. The tropical ocean monsoon climate, characterized by high temperatures and heavy precipitation, may lead to the leaching of surface PTEs (Wang AT et., 2018). Among the 12 PTEs studied, the content of seven PTEs in the topsoil samples, including Cr, Ni, Mo, V, Cu, As, and Co, exhibited a significant correlation with the subsoil samples (Fig. 4). This suggests that the content of these elements is largely determined by the soil formation process. On the other hand, Cd, Hg, Pb, Zn, and Sb in surface soil showed no significant correlation with their concentrations in the deep soil. This lack of correlation implies that these elements are more likely to be influenced by supergene geological processes and human activities. Furthermore, the CEF plays a crucial role in understanding the extent of PTE enrichment in soil during the soil formation process (Ansari AA et al., 2000). According to the CEF values, all 12 PTEs were enriched to varying degrees in the soil (Fig. 5). Cd and Hg exhibited higher CEF values than other elements, particularly in the paddy fields and dry land, indicating a significant impact of human activities on these elements. Previous studies have suggested that agricultural practices such as tobacco and rice cultivation contribute to increased Cd content in soil (Deng Y et al.,2019; Liu HW et

Table 3. Mean concentrations of PTEs in the topsoil and subsoil samples across various land-use areas in the Sanya region (mg/kg).

Index	Orchard (*n*=21)		Dry field (*n*=11)		Woodland (*n*=6)		Garden plot (*n*=21)		Paddy field (*n*=5)		Agricultural land (*n*=64)		Hainan
	Topsoil	Subsoil	Topsoil	Subsoil	Topsoil	Subsoil	Topsoil	Subsoil	Topsoil	Subsoil	Topsoil	Subsoil	Topsoil
As	3.24	11.53	3.94	5.15	4.36	3.38	3.05	5.23	8.29	8.25	3.80	7.34	1.14
Cd	0.065	0.090	0.066	0.060	0.042	0.035	0.046	0.033	0.085	0.036	0.059	0.057	0.050
Hg	0.034	0.029	0.037	0.031	0.033	0.024	0.053	0.042	0.040	0.033	0.041	0.033	0.030
Cu	6.48	8.13	7.14	7.70	6.58	12.56	6.34	8.54	10.96	10.72	6.90	8.81	4.95
Pb	27.54	44.72	28.85	27.03	31.18	31.15	26.38	29.67	33.26	37.88	28.17	34.94	22.34
Zn	39.23	61.93	50.60	49.96	31.03	46.62	45.40	59.12	54.44	47.96	43.63	56.43	35.11
Co	4.22	5.23	5.52	5.55	4.56	4.57	5.15	9.77	6.63	4.80	4.97	6.68	3.33
Cr	13.56	22.31	20.64	24.02	13.08	15.24	15.34	21.98	22.37	30.44	16.00	22.47	15.24
Ni	3.78	6.19	5.55	8.27	3.91	6.71	3.76	6.30	6.19	7.41	4.28	6.73	4.12
Mo	1.03	1.38	1.11	1.41	1.61	2.77	1.26	1.71	1.59	2.35	1.22	1.70	0.50
Sb	0.23	0.44	0.19	0.17	0.23	0.21	0.20	0.22	0.62	0.55	0.24	0.31	0.18
V	23.57	46.67	35.84	52.38	53.57	58.12	37.05	74.04	34.34	41.88	33.75	57.33	29.73
Corg	0.81	0.14	0.92	0.16	0.92	0.15	0.99	0.18	0.69	0.14	0.89	0.16	–
pH	6.24	6.13	6.14	6.03	5.99	6.08	5.58	5.63	6.22	5.98	5.98	5.93	–

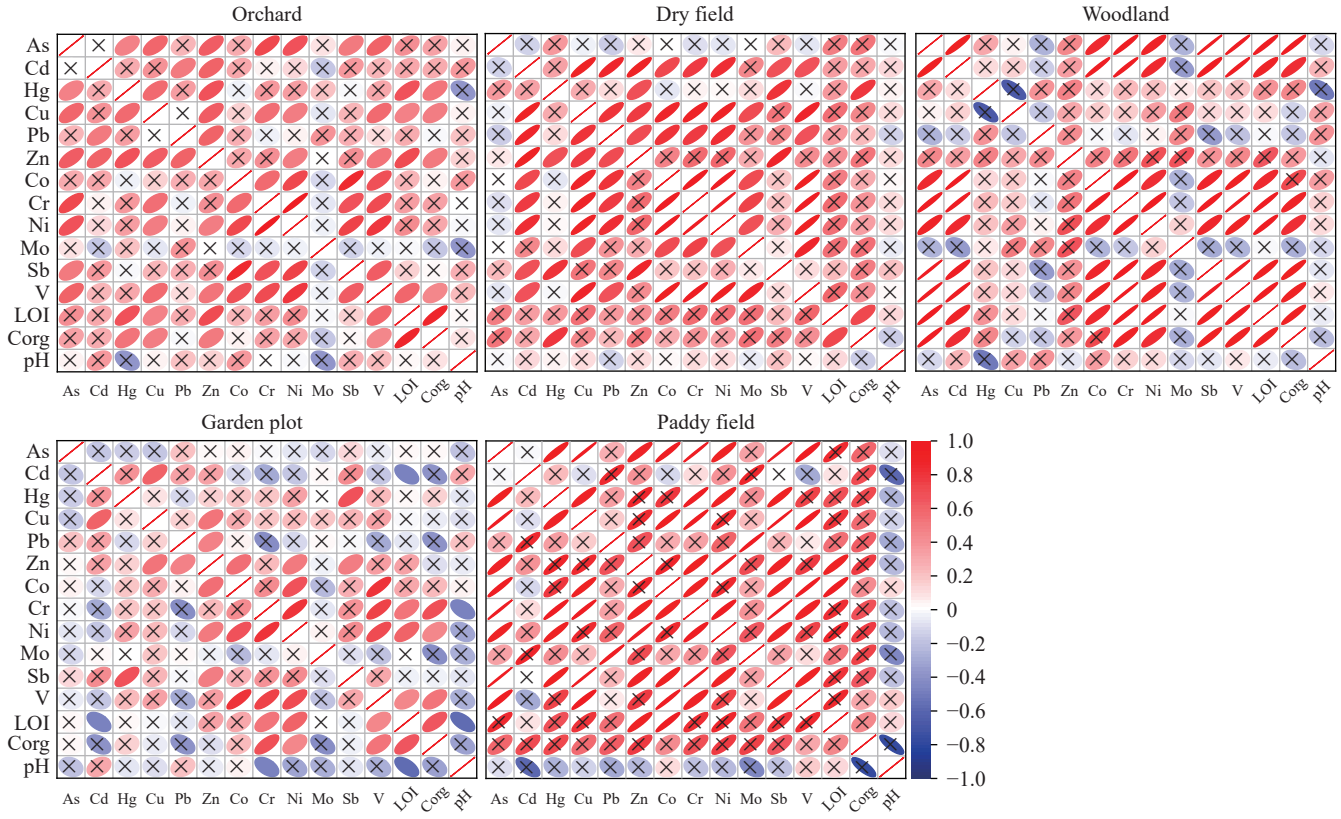

Fig. 2. Pearson correlation coefficients between PTEs and selected soil properties (Significant at the 0.05 level. The black cross indicates no correlation between the PTEs and soil components).

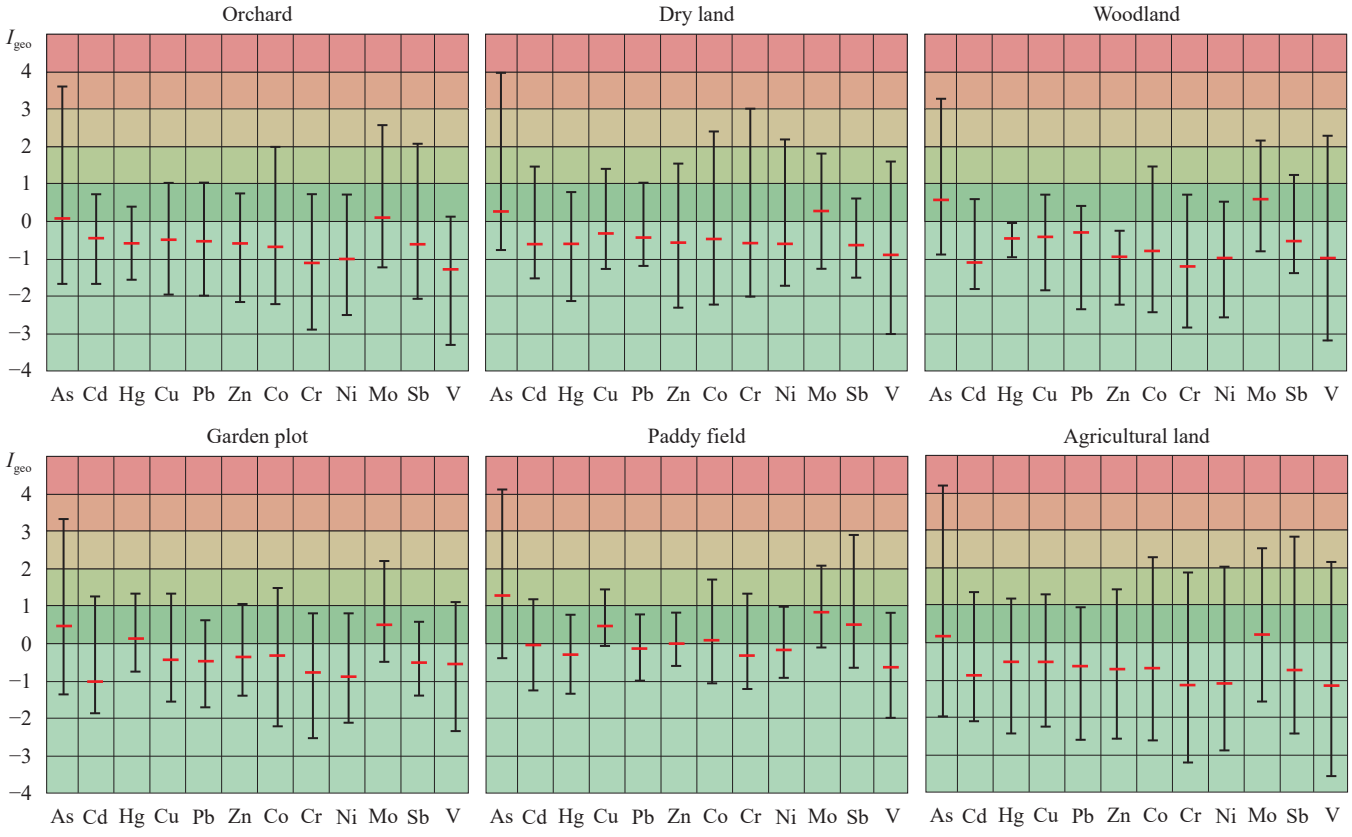

Fig. 3. Mean, minimum, and maximum I_{geo} values in different land-use areas of the Sanya region.

al., 2021). In contrast, most of the remaining PTEs, such as Cu, Cr, and Ni, showed lower median CEF values (<2, Fig. 5), suggesting that these elements primarily originated from non-polluted soil-forming parent materials. The CEF values for As

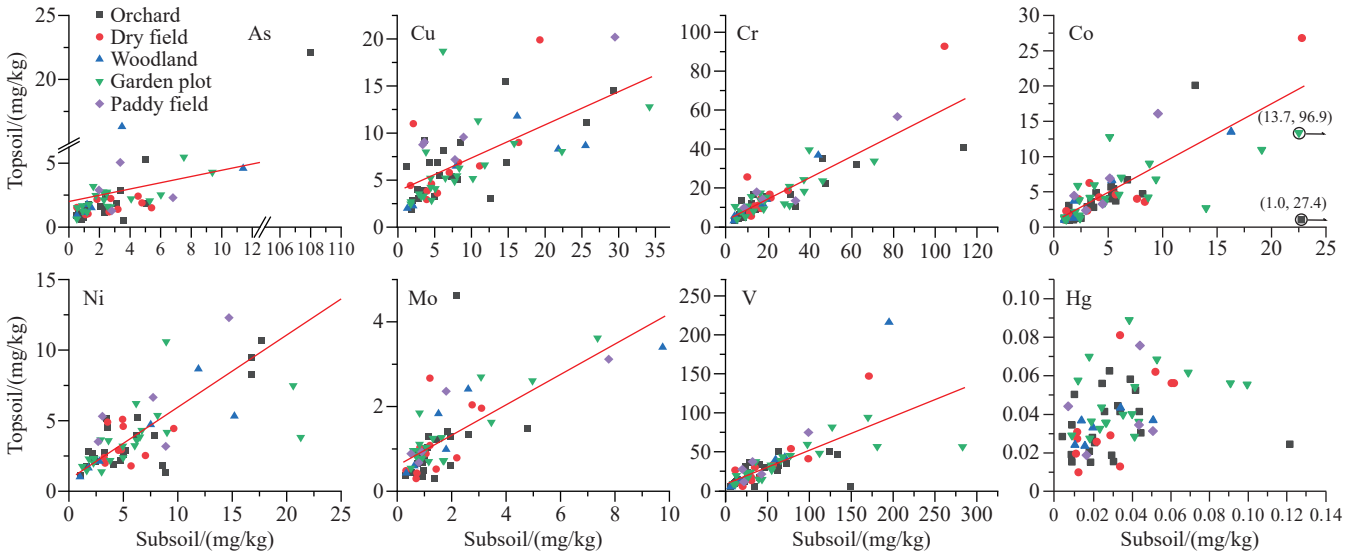

Fig. 4. Concentration of select PTEs in the topsoil and subsoil samples across various land-use areas in the Sanya region.

and V in the paddy fields and dry fields were relatively lower, indicating that these land utilization patterns might lead to the loss of As and V from the soil.

5.3. Indication of factor analysis on the source of soil PTEs

Analyzing the sources of PTEs in soil is crucial for gaining insights into the geochemical processes and identifying the origins of soil pollution (Wang AT et al., 2018; Ali L et al., 2019). Soil PTEs primarily have two main sources: The background source inherited from soil parent materials and external sources resulting from natural and human factors, including atmospheric and hydrospheric interactions as well as human activities (Wang AT et al., 2018; Ali L et al., 2019; Fei XF et al., 2020). Factor analysis is an effective tool for discerning the sources of PTEs in soil, allowing for the characterization and quantification of each pollution source's contribution.

In this study, the Kaiser-Meyer-Olkin (KMO) sampling yielded an appropriate value of 0.631 (greater than 0.5), and Bartlett's sphericity test resulted in a statistic of 533 with a p-value less than 0.05, affirming the suitability of factor analysis for achieving meaningful results. Factor analysis was applied to 64 topsoil samples standardized by maximum variance. The analysis extracted factors with characteristic roots exceeding 1, which were subsequently rotated to generate a principal component matrix, as depicted in Fig. 6. These principal components captured the information contained in the original 12 varieties of PTEs, with the cumulative variance contribution rate reaching 68.2% for the extracted components.

The first group of elements —Co, Cr, Ni, and V —exhibited substantial loadings on Factor 1, with coefficients surpassing 0.85. These transition elements share similar geochemical behaviors during weathering processes, with their contents largely influenced by the distribution of basic rocks (Wang AT et al., 2018). In agricultural practices, it is common to find that the levels of Cr and Ni in both organic and chemical fertilizers are typically lower than those present in the soil background (Qishlaqi A et al., 2009; Lv JS, 2019). However, it should be noted that the widespread presence of basalt in the region can serve as a potential source for Cr, Ni, Co, and V (Hainan Institute of Geological Survey, 2017). Consequently, Factor 1 was employed to symbolize the contribution of soil parent materials to the PTEs, constituting 30.4% of the overall sources of these elements.

The second group encompassing Pb, Cd, and Zn exhibited load coefficients on Factor 2 exceeding 0.75. Commonly employed organic fertilizers in agricultural production in Sanya, such as calcium, magnesium phosphate, cake fertilizer, and tropical crop-specific fertilizers, contained higher Cd, Pb, and Zn levels compared to the soil background (Liu HW et al., 2021; Zhao W et al., 2017). Consequently, fertilization practices inevitably elevated PTE levels in the soil. Furthermore, these three elements showed no significant correlations with either topsoil or deep soil. Hence, Factor 2 was identified as representative of the input source from agricultural activities, contributing 20.8% to the PTEs.

The third group of elements, As, Hg, and Sb, exhibited prominent load coefficients on Factor 3 (Fig. 6). Previous studies on urban and suburban soils have linked elevated Hg content in topsoil to urbanization processes, while the use of fossil fuels and atmospheric deposition contributed to increased As and Hg levels in the soil (Sun YB et al., 2010; He YS, 2014). Additionally, a significant number of samples demonstrated high CEF values for As, Hg, and Sb, with CEF values for soil parent material sources typically below 2 (Qishlaqi A et al., 2009; Wang AT et al., 2018). As a result, Factor 3 was designated to represent inputs from other human activities and atmospheric deposition, contributing 10% to the sources of PTEs.

5.4. Assessment of health risks

The assessment of health risks stemming from PTEs in the study area reveals notable insights. Calculations of ADD for both adults and children indicate that oral intake significantly surpasses dermal absorption, with children exhibiting higher

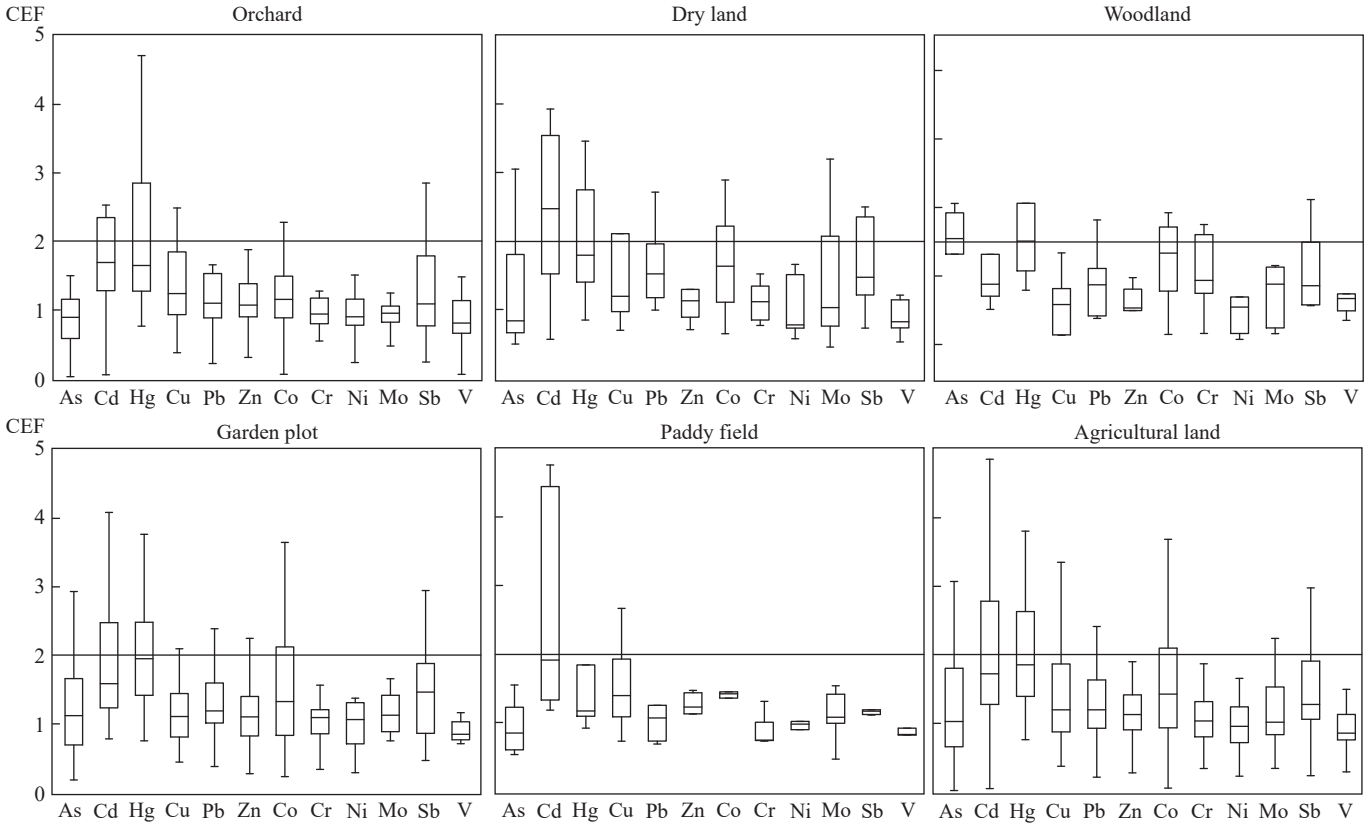

Fig. 5. CEF values in different land-use areas of the Sanya region.

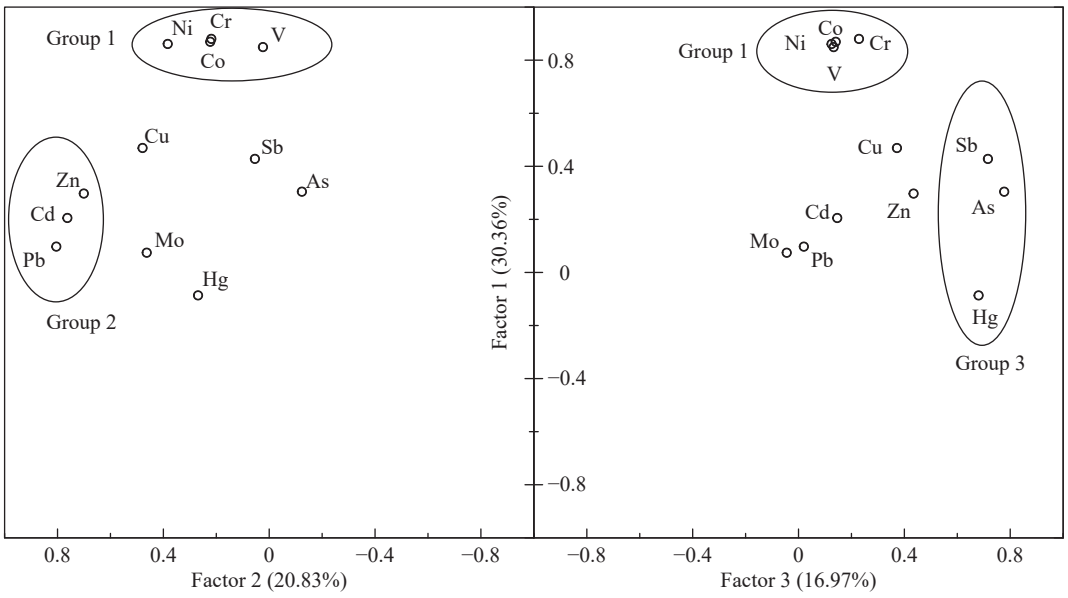

Fig. 6. Factor loading diagram of PTEs in the agricultural soil of Sanya City. Extraction method: Principal component analysis. Rotation method: Varimax with Kaiser normalization.

intake levels than adults (Table 4). The average order of oral intake for both groups is as follows: Zn > V > Pb > Cr > Cu > Co > Ni > As > Mo > Sb > Cd > Hg. Notably, there is substantial variation in the oral intake of PTEs, with Hg intake as low as 5.0×10^{-8} mg/kg/d and Zn intake reaching up to 6.6×10^{-4} mg/kg/d. Paddy fields exhibit significantly higher ADD values compared to the other four land-use types. In particular, ADD values for As and Sb are more than double those of other agricultural lands, while Cd, Hg, Cu, Pb, Zn, Mo, Co, Cr, Ni, and V show values one to two times higher.

The primary routes of non-carcinogenic element absorption by the human body are through food consumption, play activities, and walking. HQ calculations indicate that oral intake accounts for 69.2% to 99.6% of the total non-carcinogenic risk for adults, with an even higher proportion for children, ranging from 92.6% to 99.9%. These findings align with prior studies (Fryer M et al., 2006; Qu CS et al., 2012; Li ZY et al., 2014). Five elements, namely As, Ni, V,

Mo, and Cd, contribute to over 96% of the HQ value. The non-carcinogenic risk levels in all five types of agricultural lands (paddy fields, dry land, woodland, garden plots, and orchards) exceed the risk values based on the Hainan baseline (Fig. 7), indicating an elevation in non-carcinogenic risks due to agricultural activities. However, for adults, the average HQ values across all land types do not exceed 0.14 (Fig. 7), suggesting no non-carcinogenic risks. Children, due to their physiological and behavioral characteristics, exhibit higher sensitivity to pollutants per unit weight and are more likely to ingest soil particles while playing and walking (Gabarrón M et al., 2017; Qu CS et al., 2012). Nevertheless, even in paddy fields, which pose the highest risk coefficient for children, the HQ value remains only 0.9, indicating no significant non-carcinogenic risks associated with topsoil in Sanya 's agricultural lands.

The severity of carcinogenic risks posed by elements in the topsoil of Sanya's agricultural lands ranks as follows: Cr > As > Cd > Pb (Table 5). Among these, As and Cr in paddy fields and As and Cr in dry land present significantly higher carcinogenic risks than other elements, warranting particular attention. However, the carcinogenic risks associated with all 12 PTEs in soil samples are considered acceptable based on reference values. The Total Carcinogenic Risk Index (TR) for agricultural lands follows this order: Paddy fields > dry land > woodland > garden plots > orchards, all exceeding the TR value calculated using the Hainan baseline. This indicates that agricultural activities elevate soil-related carcinogenic risks. However, when compared to reference values (Yin YM et al., 2018), the overall carcinogenic risks posed by the soil in the research area remain at a low level.

Table 4. Average values of carcinogenic risks index and total health risk index in the topsoil samples ($\times10^{-6}$).

	Orchard	Dry field	Forest	Garden plot	Paddy field	Agricultural land	Hainan
As	8.58	10.46	11.51	8.09	21.82	9.98	2.89
Cd	1.65	1.65	1.05	1.20	2.10	1.50	1.27
Pb	0.40	0.41	0.45	0.38	0.48	0.41	0.32
Cr	11.46	17.43	11.06	12.96	18.93	13.52	12.9
TR	22.09	29.96	24.07	22.63	43.33	25.41	17.4

Note: The CR value of Hainan was estimated according to the Hainan soil geochemical baseline.

6. Conclusions

(i) The average content of PTEs in the topsoil for the five types of agricultural land in Sanya was higher than the baseline value of Hainan Island. The content of Cd and Hg in the topsoil was higher than in the deep soil, while the content of As, Cu, Pb, Zn, Co, Cr, Ni, Mo, Sb, and V in the topsoil was lower than in the deep soil.

(ii) Geological statistics indicate varying degrees of accumulation for As and Mo across all agricultural land types. Notably, Cu, Co, and Sb accumulate to higher extents in paddy fields, while Hg accumulates more in garden plots. Source identification results highlight that Cr, Ni, Mo, V, Cu, As, and Co content in the soil primarily results from soil formation processes, while Cd, Hg, Pb, Zn, and Sb are influenced to a greater extent by supergene environmental factors and human activities. Among these, soil parent materials and agricultural practices emerge as major contributors to PTEs in the topsoil.

(iii) The assessment of health risks, relative to the Hainan baseline, indicates varying degrees of non-carcinogenic and carcinogenic risks posed by the soil to human health across the five land utilization types, with the severity ranking as follows: paddy fields > dry land > woodland > garden plots > orchards. Nevertheless, it is crucial to note that the soil in these five land utilization types presents only minimal risks to human health.

CRediT authorship contribution statement

Jian-zhou Yang and Jing-Jing Gong conceived of the presented idea. Jian-zhou Yang and Yan-gang Fu wrote the manuscript with support from Qiu-li Gong and Sheng-ming Ma. All authors discussed the results and contributed to the final manuscript.

Declaration of competing interest

The authors declare no conflict of interest.

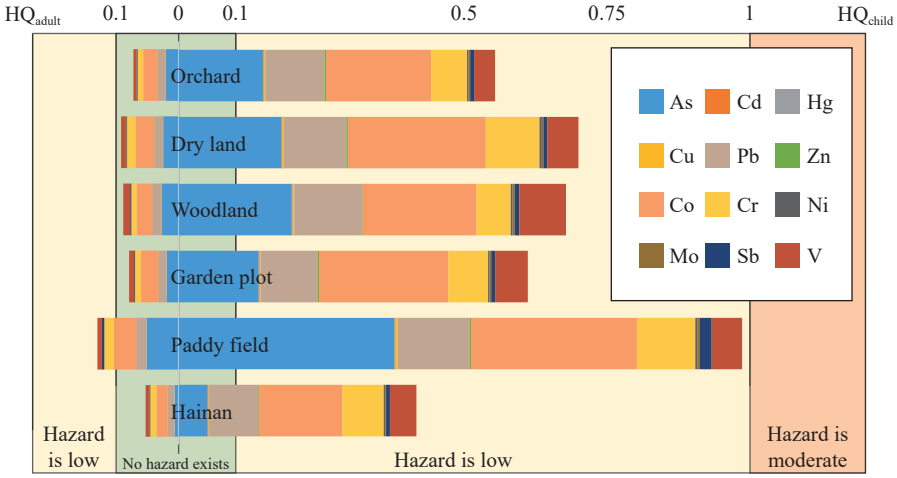

Fig. 7. Plot of the HQ for adults and children in five land-use zones of the Sanya region (The HQ value for Hainan was estimated based on the geochemical baseline of PTEs in Hainan Province).

Table 5. Average daily doses of ingestion and dermal contact with soils based on total PTE concentrations for adults and children in different land-use areas of Sanya ($\times10^{-6}$).

PTE		Orchard		Dry field		Forest		Garden		Paddy field		Agricultural land	
		ADD_{ingest}	ADD_{dernal}	ADD_{ingest}	ADD_{dernal}	ADD_{ingest}	ADD_{dernal}	ADD_{ingest}	ADD_{dernal}	ADD_{ingest}	ADD_{dernal}	ADD_{ingest}	ADD_{dernal}
As	Adult	5.5	0.8	6.7	1	7.4	1	5.2	0.7	14	2	6.4	0.93
	Child	39	1.5	47.6	1.8	52.5	2	36.8	1.4	99.9	3.9	45.8	1.78
Cd	Adult	0.11	0.001	0.11	0.001	0.07	0.0003	0.08	0.0004	0.14	0.001	0.1	0.0005
	Child	0.80	0.001	0.80	0.001	0.50	0.001	0.60	0.001	1.01	0.001	0.70	0.0009
Hg	Adult	0.06	0.0003	0.06	0.0003	0.05	0.0003	0.09	0.0004	0.07	0.0003	0.07	0.34
	Child	0.40	0.001	0.40	0.001	0.40	0.001	0.60	0.001	0.50	0.001	0.50	0.64
Cu	Adult	10.9	0.05	12.1	0.06	11.1	0.05	10.7	0.05	18.5	0.09	11.7	0.06
	Child	78.1	0.1	86.1	0.1	79.3	0.1	76.4	0.1	132	0.2	83.1	0.1
Pb	Adult	46.5	0.2	48.7	0.2	52.6	0.3	44.5	0.2	56.1	0.3	47.6	0.23
	Child	332	0.4	348	0.5	376	0.5	318	0.4	401	0.2	340	0.44
Zn	Adult	66.2	0.3	85.4	0.4	52.4	0.3	76.6	0.4	91.9	0.4	73.7	0.36
	Child	473	0.6	610	0.8	374	0.5	548	0.7	657	0.9	526	0.68
Co	Adult	7.12	0.03	9.31	0.04	7.69	0.04	8.7	0.04	11.2	0.05	8.39	0.04
	Child	50.8	0.1	66.5	0.1	54.9	0.1	62.1	0.1	80	0.1	60	0.08
Cr	Adult	22.9	0.1	34.8	0.2	22.1	0.1	25.9	0.1	37.8	0.2	27	0.13
	Child	164	0.2	249	0.3	158	0.2	185	0.2	270	0.3	193	0.25
Ni	Adult	6.4	0.03	9.4	0.05	6.6	0.03	6.3	0.03	10.5	0.05	7.2	0.04
	Child	45.5	0.06	67	0.09	47.2	0.06	45.3	0.06	74.7	0.1	51.6	0.07
Mo	Adult	1.7	0.008	1.9	0.009	2.7	0.013	2.1	0.01	2.7	0.01	2.1	0.01
	Child	12.4	0.016	13.4	0.017	19.4	0.025	15.2	0.02	19.2	0.02	14.7	0.02
Sb	Adult	0.4	0.02	0.3	0.02	0.4	0.02	0.3	0.02	1	0.05	0.4	0.002
	Child	2.8	0.004	2.3	0.003	2.7	0.004	2.4	0.003	7.5	0.01	2.9	0.004
V	Adult	39.8	0.2	60.5	0.3	90.4	0.4	62.6	0.3	58	0.3	57	0.28
	Child	284	0.4	432	0.6	646	0.8	447	0.6	414	0.5	407	0.53

Acknowledgment

This work was supported by Open Foundation of the Key Laboratory of Coupling Process and Effect of Natural Resources Elements (No.2023KFKTB001), the Science & Technology Fundamental Resources Investigation Program (2022FY101800), the National Nonprofit Institute Research Grant of IGGE (AS2023D01), the projects of the China Geological Survey (DD20230309 and DD20190305), and the National Natural Science Foundation of China (42002105).

References

Ali L, Rashid A, Khattak SA, Zeb M, Jehan S. 2019. Geochemical control of potential toxic elements (PTEs), associated risk exposure and source apportionment of agricultural soil in Southern Chitral, Pakistan. Microchemical Journal, 147, 516–523. doi: 10.1016/j.microc.2019.03.034.

Ansari AA, Singh IB, Tobschall HJ. 2000. Importance of geomorphology and sedimentation processes for metal dispersion in sediments and soils of the Ganga Plain: Identification of geochemical domains. Chemical Geology, 162(3), 245–266. doi: 10.1016/S0009-2541(99)00073-X.

Bao LR, Deng H, Jia ZM, Li Y, Dong JX, Yan MS, Zhang FL. 2020. Ecological and health risk assessment of heavy metals in farmland soil of northwest Xiushan, Chongqing. Geology in China, 47(6), 1625–1636 (in Chinese with English abstract). doi: 10.12029/gc20200602.

Bloom PR. 1996. Environmental chemistry of soils. Soil Science, 161(1), 70–71. doi: 10.1097/00010694-199601000-00009.

Braun JJ, Pagel M, Herbilln A, Rosin H. 1993. Mobilization and redistribution of REEs and thorium in a syenitic lateritic profile: A mass balance study. Geochimica et Cosmochimica Acta, 57(18), 4419–4434. doi: 10.1016/0016-7037(93)90492-F.

Cai LM, Wang QS, Wen HH, Luo J, Wang S. 2019. Heavy metals in agricultural soils from a typical township in Guangdong China: Occurrences and spatial distribution. Ecotoxicology and Environmental Safety, 168, 184–191. doi: 10.1016/j.ecoenv.2018.10.092.

Cao SZ, Duan XL, Zhao XG, Ma J, Wei FS. 2013. Health risks from the exposure of children to As, Se, Pb and other heavy metals near the largest coking plant in China. Science of the Total Environment, 472C, 1001–1009. doi: 10.1016/j.scitotenv.2013.11.124.

Deng Y, Jiang LH, Xu LF, Hao XD, Zhang SY, Xu ML, Zhu P, Fu SD, Liang YL, Yin HQ, Liu XD, Bai LY, Jiang HD, Liu HW. 2019. Spatial distribution and risk assessment of heavy metals in contaminated paddy fields – A case study in Xiangtan City, southern China. Ecotoxicology and Environmental Safety, 171, 281–289. doi: 10.1016/j.ecoenv.2018.12.060.

Fei XF, Xiao R, Christakos G, Langousis A, Ren ZQ, Tian Y, Lv XN. 2019. Comprehensive assessment and source apportionment of heavy metals in Shanghai agricultural soils with different fertility levels. Ecological indicators, 106, 105508. doi: 10.1016/j.ecolind.2019.105508.

Fei XF, Lou ZH, Xiao R, Ren ZQ, Lv XN. 2020. Contamination assessment and source apportionment of heavy metals in agricultural soil through the synthesis of PMF and GeogDetector models. Science of the Total Environment, 747, 141293. doi: 10.1016/j.scitotenv.2020.141293.

Fergusson JE. 1990. The Heavy Elements: Chemistry, Environmental Impact and Health. Oxford,Pergamon Press, 614.

Fryer M, Collins CD, Ferrier H, Colvile RN, Nieuwenhuijsen MJ. 2006. Human exposure modelling for chemical risk assessment: A review of current approaches and research and policy implications. Environmental Science & Policy, 9(3), 261–274. doi: 10.1016/j.envsci.2005.11.011.

Fu YR, Yang Y, He YS, Zhang GC, Ma RL, Xie SZ, Liu HF, Guo YP,

Xia N, Fu XL, Mo WR, Wang F, Xue GC, Chen YW. 2008. Multi–purpose Regional Geochemical Report of Hainan Island. Haikou, Hainan Institute of Geological Survey, 69–70 (in Chinese).

Gabarrón M, Faz A, Acosta JA. 2017. Soil or dust for health risk assessment studies in urban environment. Archives of Environmental Contamination & Toxicology, 73, 442–455. doi: 10.1007/s00244-017-0413-x.

Geng N, Wu YC, Zhang M, Tsang DCW, Rinklebe J, Xia YF, Lu DB, Zhu LF, Palansooriya KN, Kim K, Ok YS. 2019. Bioaccumulation of potentially toxic elements by submerged plants and biofilms: A critical review. Environment International, 131, 105015. doi: 10.1016/j.envint.2019.105015.

Hainan Institute of Geological Survey. 2017. Regional geology of China, Hainan Province. Beijing, Geological Publishing House, 908 (in Chinese).

He YS. 2014. Pollution characteristics and ecological risk assessment of heavy metals in Haikou urban soils. Journal of Ecology, 33(2), 421–428 (in Chinese with English abstract). doi: 10.13292/j.1000-4890.2014.0024.

Hill IG, Worden RH. 2000. Yttrium: The immobility-mobility transition during basaltic weathering. Geology, 28(10), 923–926. doi: 10.1130/0091-7613(2000)28<923:YTITDB>2.0.CO;2.

Kasimov N, Kosheleva N, Gunin P, Korlyakov I, Sorokina O, Timofeev I. 2016. State of the environment of urban and mining areas in the Selenga Transboundary River Basin (Mongolia Russia). Environmental Earth Sciences, 75(18), 1281–1283. doi: 10.1007/s12665-016-6088-1.

Kim HS, Kim YJ, Seo YR. 2015. An overview of carcinogenic heavy metal: molecular toxicity mechanism and prevention. Journal of Cancer Prevention, 20(4), 232–240. doi: 10.15430/JCP.2015.20.4.232.

Kurtz AC, Derry LA, Chadwick OA, Alfano MJ. 2000. Refractory element mobility in volcanic soils. Geology, 28(28), 279–282. doi: 10.1130/0091–7613(2000)0282.3.CO;2.

Li ZY, Ma ZW, van der Kuijp TJ, Yuan ZW, Huang L. 2014. A review of soil heavy metal pollution from mines in China: Pollution and health risk assessment. Science of the Total Environment, 468–469, 843–853. doi: 10.1016/j.scitotenv.2013.08.090.

Liu HW, Wang HY, Zhang Y, Yuan JM, Peng YD, Li XC, Shi Y, He KX, Zhang QM. 2018. Risk assessment, spatial distribution, and source apportionment of heavy metals in Chinese surface soils from a typically tobacco cultivated area. Environmental Science and Pollution Research, 25(17), 16852–16863. doi: 10.1007/s11356-018-1866-9.

Liu HW, Zhang Y, Yang JS, Wang HY, Li YL, Shi Y, Li DC, Holm PE, Ou Q, Hu WY. 2021. Quantitative source apportionment, risk assessment and distribution of heavy metals in agricultural soils from southern Shandong Peninsula of China. Science of the Total Environment, 767, 144879. doi: 10.1016/j.scitotenv.2020.144879.

Lv JS. 2019. Multivariate receptor models and robust geostatistics to estimate source apportionment of heavy metals in soils. Environmental Pollution, 244, 72–83. doi: 10.1016/j.envpol.2018.09.147.

Means B. 1989. Risk–assessment guidance for Superfund. Volume 1. Human Health Evaluation Manual. Part A. Interim report (Final). United States.

Memoli V, Esposito F, Panico SC, De Marco A, Barile R, Maisto G. 2019. Evaluation of tourism impact on soil metal accumulation through single and integrated indices. Science of the Total Environment, 682, 685–691. doi: 10.1016/j.scitotenv.2019.05.211.

MEP (Ministry of Environmental Protection). 2014. HJ 25.3–2014, Technical guidelines for risk assessment of contaminated sites (in Chinese).

Micó C, Recatalá L, Peris M, Sánchez J. 2006. Assessing heavy metal sources in agricultural soils of an European Mediterranean area by multivariate analysis. Chemosphere, 65(5), 863–872. doi: 10.1016/j.chemosphere.2006.03.016.

Muller G. 1969. Index of geoaccumulation in sediments of the Rhine river. Geojournal, 2(3), 109–118.

Nesbitt HW. 1979. Mobility and fractionation of rare earth elements during weathering of a granodiorite. Nature, 279(5710), 206–210. doi: 10.1038/279206a0.

Pourret O, Bollinger JC. 2018. “Heavy metal” – What to do now: To use or not to use? Science of the Total Environment, 610–611, 419–420. doi: 10.1016/j.scitotenv.2017.08.043.

Qishlaqi A, Moore F, Forghani G. 2009. Characterization of metal pollution in soils under two landuse patterns in the Angouran region, NW Iran; a study based on multivariate data analysis. Journal of Hazardous Materials, 172(1), 374–384. doi: 10.1016/j.jhazmat.2009.07.024.

Qu CS, Sun K, Wang SR, Huang L, Bi J. 2012. Monte carlo simulation–based health risk assessment of heavy metal soil pollution: a case study in the Qixia mining area, China. Human and Ecological Risk Assessment: An International Journal, 18(4), 733–750. doi: 10.1080/10807039.2012.688697.

Reimann C, Kashulina G, Caritat PD, Niskavaara H. 2001. Multi-element, multi-medium regional geochemistry in the European arctic: element concentration, variation and correlation. Applied Geochemistry, 16(7), 759–780. doi: 10.1016/S0883-2927(00)00070-6.

RSL, 2017. Regional Screening Levels – Generic Tables.

Sun YB, Zhou QX, Xie XK, Liu R. 2010. Spatial, sources and risk assessment of heavy metal contamination of urban soils in typical regions of Shenyang, China. Journal of Hazardous Materials, 174(1), 455–462. doi: 10.1016/j.jhazmat.2009.09.074.

Timofeev I, Kosheleva N. 2017. Geochemical disturbance of soil cover in the nonferrous mining centers of the Selenga River basin. Environmental Geochemistry and Health, 39(4), 803–819. doi: 10.1007/s10653–016–9850–0.

Timofeev I, Kosheleva N, Kasimov N. 2019. Health risk assessment based on the contents of potentially toxic elements in urban soils of Darkhan, Mongolia. Journal of Environmental Management, 242, 279–289. doi: 10.1016/j.jenvman.2019.04.090.

USEPA. 2002. Supplemental guidance for developing soil screening levels for superfund sites. vol. 106.

Wang AT, Wang Q, Li J, Yuan GL, Albanese S, Petrik A. 2018. Geo–statistical and multivariate analyses of potentially toxic elements ’ distribution in the soil of Hainan Island (China): A comparison between the topsoil and subsoil at a regional scale. Journal of Geochemical Exploration. 197, 48–59. doi: 10.1016/j.gexplo.2018.11.008.

Wang FF, Guan QY, Tian J, Lin JK, Yang YY Yang LQ, Pan NH. 2020. Contamination characteristics, source apportionment, and health risk assessment of heavy metals in agricultural soil in the Hexi Corridor. Catena (Giessen), 191, 104573. doi: 10.1016/j.catena.2020.104573.

Yang SH, Qu YJ, Ma J, Liu LL, Wu HW, Liu QY, Gong YW, Chen YX, Wu YH. 2020. Comparison of the concentrations, sources, and distributions of heavy metal (loid)s in agricultural soils of two provinces in the Yangtze River Delta, China. Environmental Pollution, 264, 114688. doi: 10.1016/j.envpol.2020.114688.

Yin YM, Zhao WT, Huang T, Cheng SG, Zhao ZL, Yu CC. 2018. Distribution characteristics and health risk assessment of heavy metals in a soil–rice system in an E–waste Dismantling area. Environmental Science, 39(2), 916–926 (in Chinese with English abstract). doi: 10.13227/j.hjkx.201704122.

Zhang Q, Bai JF, Wang Y. 2012. Analytical scheme and quality monitoring system for China Geochemical Baselines. Earth Science Frontiers, 19(3), 33–42 (in Chinese with English abstract). doi: 10.1007/s11783-011-0280-z.

Zhang XW, Yang LS, Li YH, Li HR, Wang WY, Ye BX. 2012. Impacts of lead/zinc mining and smelting on the environment and human health in China. Environmental Monitoring & Assessment, 184(4), 2261–2273. doi: 10.1007/s10661–011–2115–6.

Zhao W, Pan YZ, Lan T, Wu ZP, Zhang LL, Zhu ZQ, Wu WD. 2017. Analysis of heavy metals and antibiotics content in Hainan commercial organic fertilizers. Environmental Chemistry, 36(2), 408–419 (in Chinese with English abstract). doi: 10.7524/j.issn.0254-6108.2017.02.2016051803.